IS-PORTO 2023 PROCEEDINGS

Proceedings of the 8th International Symposium on DEFORMATION CHARACTERISTICS OF GEOMATERIALS Porto, 3rd - 6th September 2023

Effects of vegetation on the hydro-mechanical properties of the vadose zone

Floriana Anselmucci[1#], *Hongyang* Cheng[1], *Xinyan* Fan[2], *Yijian* Zeng[3] and *Vanessa* Magnanimo[1]

[1]*Department of Civil Engineering, Faculty of Engineering Technology, MESA+, University of Twente, P.O. Box 217, 7500 AE Enschede, The Netherlands*

[2]*Department of Natural Resources, Faculty of Geo-information Science and Earth Observation, University of Twente P.O. Box 217, 7500 AE Enschede, the Netherlands*

[3]*Department of Water Resources, Faculty of Geo-information Science and Earth Observation, University of Twente P.O. Box 217, 7500 AE Enschede, the Netherlands*

[#]*Corresponding author: f.a.r.anselmucci@utwente.nl*

ABSTRACT

The hydro-mechanical properties of the vadose zone are strongly influenced by seasonal cycles. The hydraulic behavior of this zone is determined by the coupling of biotic and abiotic factors. The biotic factors are controlled by the physiology and anatomy of the vegetation growing in the area, while the abiotic factors depend on the local soil characteristics, such as water content, void ratio, and matrix structure. In this laboratory-scale investigation, we assess the influence of active biomass, water content, and suction on the particle and pore structure rearrangement. We use x-ray computed tomography and 3D digital image correlation to quantify plant roots at different stages of growth, soil deformation, and water content fluctuations. Our results show that the bulk porosity of vegetated soil is strongly affected by the induced water cycles. The global micro-structure rearrangement due to the double effects of plant water uptake and induced drying-wetting cycles translates into a final bulk porosity increase.

Keywords: vadose zone; vegetated soil; image processing; 3D microstructure evolution.

1. Background

Investigations of unsaturated soil at any scale aim to study the stresses, suctions, temperatures, and the history of chemical and bacterial activity in the material (Laloui, 2013).

In-situ conditions and their laboratory replicas are those typical of the vadose zone. The vadose zone is the layer of soil lying between the free surface and the water table. This layer plays a crucial role in the soil hydraulic cycle, as it is where water from precipitation infiltrates into the ground and replenishes groundwater reservoirs. It also plays a key role in the health of terrestrial ecosystems. The mechanisms occurring in the vadose zone due to water content variation are often the ones that trigger shallow slope failures (Chae and Kim, 2012; Tohari et al., 2007). Additionally, infrastructures are often buried in this part of the soil profile, and knowledge of the soil properties can help their correct installation and maintenance, as well as preventing uplifting (Byrne et al., 2013).

Soil moisture is a key variable for understanding hydrological processes in the vadose zone. The thickness of this zone can vary depending on factors such as the type of soil, the fluctuation of the water table, and the amount of vegetation in the area, as well as the specific location.

This study focuses on the influence of sudden changes in water content on partially saturated vegetated granular soil (i.e., resembling the vadose zone). A protocol for obtaining reproducible samples of sand with sprouting seeds is described. Wild type maize seeds are planted in cylindrical containers filled with sandy soil and allowed to grow for two weeks. Images from x-ray tomography are used to study the microstructure evolution and plant growth during two different water cycles in the soil. The acquired images are processed and segmented into four phases (soil, roots, pores, water), this help to quantify the influence of water variation on the pore structure.

It is well-known that the pores structure can change the retention properties of the soil. For instance, a large amount of small pores leads to higher residual saturation. If we know how water cycles affect the dimensions and spatial distribution of the pores, we can infer the soil water retention properties of the in-situ soil. This leads to a better understanding of the mechanical response of the soil to external loads.

The focus is on the evolution of pores structure and saturation because it is one of the key properties for controlling the retention properties of the soil. The evolution of soil porosity during root growth is measured, with a focus on the microstructure.

2. Experimental Campaign

It is well known that soil layers near the ground surface are partially composed of sandy soil, which has often proven to be a suitable environment for plant growth. Sand produces a porous medium that allows water (rain and groundwater) to easily percolate.

Laboratory-scale samples of vegetated sand are prepared and subjected to water cycles that simulate in-situ conditions. The effect on the soil matrix is observed through x-ray tomographies.

The sand granulometry used in this project is chosen to achieve optimal conditions for homogeneous water drainage, plant growth, and matric suction readings. Sand samples with a fairly wide particle distribution were prepared, as shown in Figure 1, allowing a significant variation in particle size within the sample.

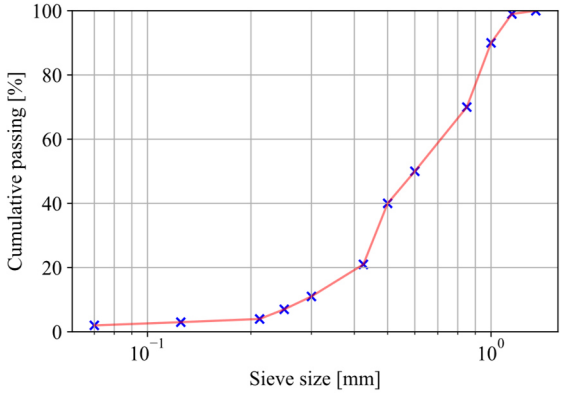

Figure 1. Built granulometric curve of the sand used.

One of the goals of the study is to observe the evolution of the soil and pore microstructure at different water contents. Therefore, the sample size is narrowed to 36 mm in diameter and 50 mm in height, as shown in Figure 2. The container is made of polymethyl methacrylate (PMMA), a transparent plastic commonly known by the brand name Plexiglass. The vegetated part of the sample is obtained using Zea L. maize seeds. Maize is one of the most widely grown crops in the world and is used as a staple food in many countries. It grows at a rate of 2-7 cm/day, even in distressed soil.

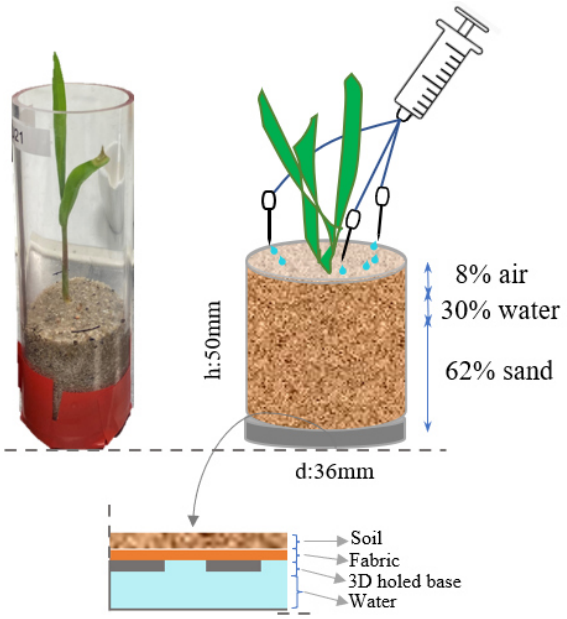

Figure 2. Representation of a typical sample used for the experimental campaign (on the left). A sketch of the volumes distribution of the medium, along with the watering technique and a zoom of the bottom container design (on the bottom right).

2.1. Induced Water cycles

Over the course of a year, the water cycle in the vadose zone can undergo significant changes in response to seasonal variations in temperature and precipitation, e.g., in the Netherlands groundwater level is particularly shallow (Colenbrander et al, 1989).

The water cycles in this study are obtained by natural evaporation for drying and direct water injection for wetting.

The range of maximum and minimum water content is determined after careful investigation to determine the range that does not stress the plants. The water content measured excludes the water stored in the base of the container. The minimum established water content is around 6%, and the maximum supported by the plant is 16%. Based on these two values, two main patterns are followed: from 6% to 16%, and vice versa, defined as the wetting and drying cycles, respectively.

2.2. Sample preparation

The protocol to prepare the sample involves several steps. This procedure is designed in order to reproduce an elementary volume of soil in-situ in the vadose zone.

- The maize seeds need to be germinated before planting. To reduce the presence of harmful microorganisms that may be present on the seeds, they are disinfected. Disinfecting seeds can help to improve their germination rate and reduce the risk of disease in the grown plants. There are several methods that can be used to disinfect seeds. In our specific case we submitted the seeds to three-cycles wash with a solution made of 15% sodium hypochlorite (NaOCl) and 85% distilled water. To remove excess of NaOCl the seeds are left to soak for 20 minutes in distilled water, and then left in waterlogged germination paper for 48 hours.
- The bottom of the sample has a double surface to allow a thin layer of water constantly in a compartment underneath the soil. This allows the bottom of the soil sample to remain at a constant humidity – as it is in-situ. The surface of the bottom cap was 3D printed, with a scheme of holes, and sealed with cotton fabric. The fabric layer allows the water to filter underneath, while keeping all the sand particles above it (Figure 2).
- Considering the sand as an inorganic soil, the water used for the samples is specifically prepared as a nutrient-rich water. The nutrients included are those essential for plant growth, such as: Nitrogen (N), Phosphorous Pentoxide (P_2O_5), Potassium Oxide (K_2O), as well as small content of Manganese (Mn), Zinc(Zn), Boron (B), Copper (Cu), and Iron (Fe).
- The soil is laid within the container through pluviation. This deposition technique helps the soil to distribute homogeneously within the container, hence, no local heterogeneity is expected.
- During pluviation, the germinated maize seed is planted at approximately 1 cm from the free surface.
- Once the dry sample is ready, the pre-established initial water content is injected in the soil. The water injection is done from the top free-surface via a

syringe with three flexible pipes to simulate rainfall and allow water percolation in the medium.

- Samples are kept in a growing chamber to a constant air humidity of 42±2% and a temperature of 22±1.5°C. The chamber is instrumented with an air extractor to provide fresh air and a cold lamp with a specific spectrum for plant growth. A day-night cycle of 16-8 hours is set.

A total of 22 samples are observed throughout two weeks post-germination. Half of the samples are subjected to a drying-wetting-drying-wetting cycle (DWDW), while the other half to a wetting-drying-wetting-drying cycle (WDWD).

A total of four samples, two assigned to each water cycle, are equipped with a moisture sensor and a tensiometer. The ET5, manufactured by Meter Group, is employed to provide measurements of the Volumetric Water Content (VWC) throughout the water cycles. In addition, the laboratory tensiometer Teros31 (Meter Group) is utilized to monitor soil water potential. The moisture sensor and tensiometer readings were used to overview the global trend of the water content and matric potential of the other – not instrumented - samples. As underlined in literature, the soil water retention curve (SWRC) is a key property to characterize the hydrological behavior of vegetated soil. When soil is subjected to water cycles, SWRCs show hysteresis.
Finally, six samples (three per each water cycle) are imaged spatially in-vivo though x-ray computed tomography. Within this paper the results of a single sample subjected to DWDW cycles are presented.

2.3. Imaging setup

While the plant is growing in the samples, x-ray tomographies are acquired for about 10 days using a tomograph at Technische Universiteit Delft (Delft, The Netherlands). During the scanning time, the container is sealed with paraffin, to keep the soil water content constant. The first tomograph is used as reference status and it is acquired before the germinated seedling could push through the sand particles. This is the initial state (t=0) used for the following analyses. Then, the paraffin is removed, the plant is let grow and water let evaporate naturally.

The tomographies are acquired every 24 hours. The duration of the acquisition is the result of a spatial and temporal resolution trade off. The voltage and current of the x-ray source are set to 110 kV and 220 µA with an exposure time of 1 second on each radiography. The scanning is performed during a 360° continuous rotation and 1440 projections are acquired, making one single tomography last 28 minutes. The final pixel-size is 22.5 µm. Each tomography is reconstructed and the analysis is detailed in the next section. In the following, the results presented refer to a binned version of the original images. The downscaling factor applied is 2, hence, the final voxel size is 45 µm.

3. Image Processing

Eight tomographies are obtained on average for each observed samples. While the reconstruction is performed using the same program and procedure, the histograms of the pixels greyvalues distribution of each image may be different. Such difference is due to the overall greyscale average assigned to the x-ray adsorption while converting the radiographies in tomographies. Prior to any histogram normalization, a bilateral filter (Tomasi and Manduchi 1998) is applied to all images. This is an image-processing filter used to reduce noise by smoothing the texture of the image, while preserving the edges. The filter uses two information based on the spatial and intensity distributions of the greyvalues. Both these information are kept constant for each set. To ensure consistent segmentation throughout the entire set of images, a linear stretching is applied to each image to create a homogeneous normalized greyvalues histogram. Figure 3 displays the difference between the original and modified histograms of the set of scans representing the chrono-evolution of the soil sample. Focusing the attention on the darker and lighter peaks, it is evident how the linear stretch normalizes and aligns the position of the peaks. This allows the usage of the same thresholds within the different images within one set. Without the

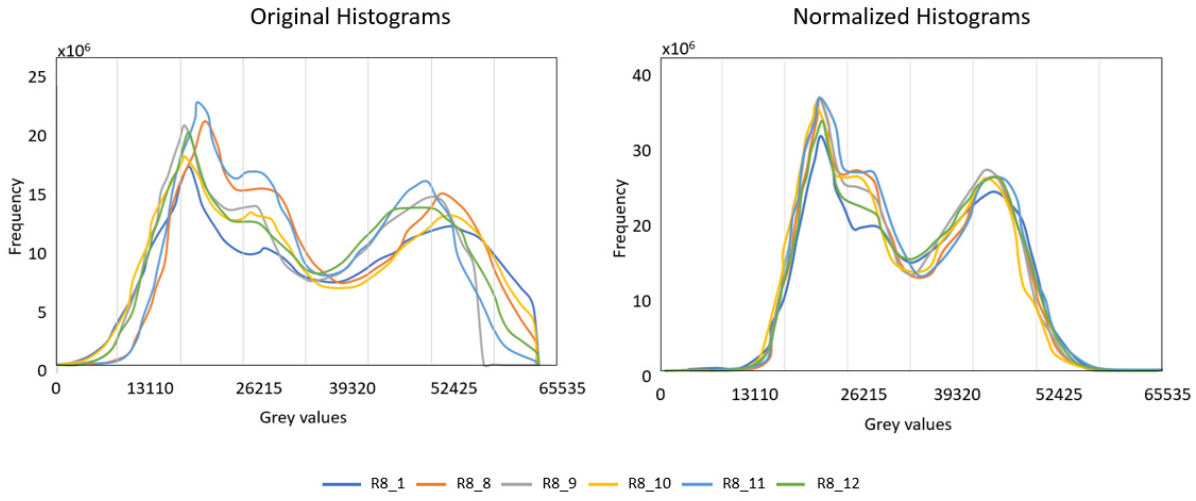

Figure 3. Comparison of histograms of the same set of tomographies related to the observed sample. On the left, the original histograms. On the right, the histograms obtained after the linear stretch. After normalization, the two main peaks of the histograms are aligned, which means that the same range of greyvalues indicates a specific phase in the image.

linear stretch, the peaks of the histograms would not have been aligned (as shown in Figure 3 left), leading to larger errors in the detection of phases (soil, water, air, roots).

3.1. Segmentation

3.1.1. Soil

The solid volume is segmented based on thresholding, which yields the exact soil fraction pluviated in the system. The threshold is set in the reference image (day 0 - germinated seed), and the same threshold is applied to the entire set of images thanks to the histogram linear stretch mentioned above. As shown in Figure 4, the soil volume fraction remains constant over time. This is expected, since there is no loss of solid material during the experiments.

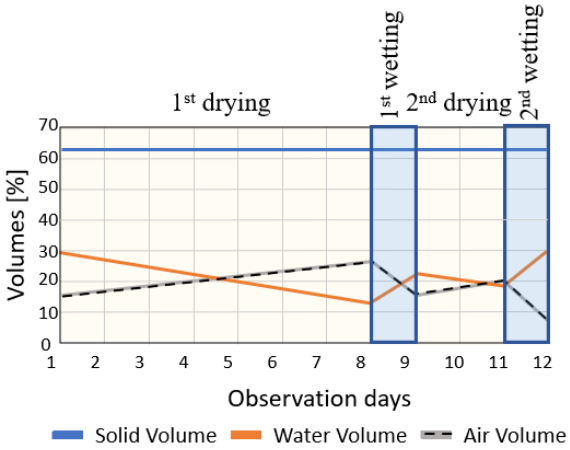

Figure 4. Volumes trend fluctuation during the observation time. Values refer to the bulk quantities extracted from the image segmentation.

3.1.2. Root system

Root system identification is obtained at each time step of the observation. The protocol used is the one presented in Anselmucci et al., 2021b. For sake of brevity, readers are referred to the cited paper for details on the procedure. Figure 5 shows the final root system within the observed sample in this study.

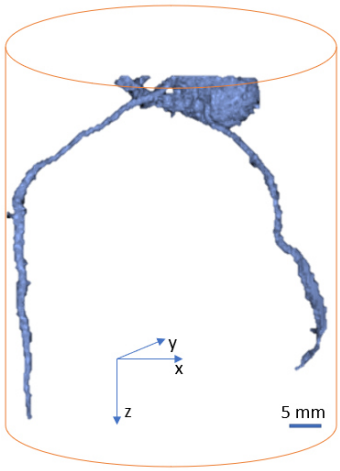

Figure 5. 3D view of the root system (10 days-old) contained in the sample subjected to DWDW water cycles.

3.1.3. Water

It is always challenging to separate the water and root phases. As explained for the segmentation of the solid phase, the water identification is obtained based on the known water weight within the unrooted reference state. By comparing the sample weights before and after the scan, we ensured that no evaporation occurred during the scan. Since the water content remained constant within the medium, the water mass is the correct validation for the water segmentation.

Starting from the greyscale image, a mask value is assigned to the pixels detected as sand and root. On the remaining (unmasked) pixels, the greyvalues threshold indicating the water is chosen based on the greyvalues giving a water volume equal to the known water content injected in the system before scanning (Anselmucci et al, 2021b). A final four-phases slice is presented in Figure 6, as an example.

The segmentation of the phases gives as well an overview of their volume variation in time, as shown in Figure 4.

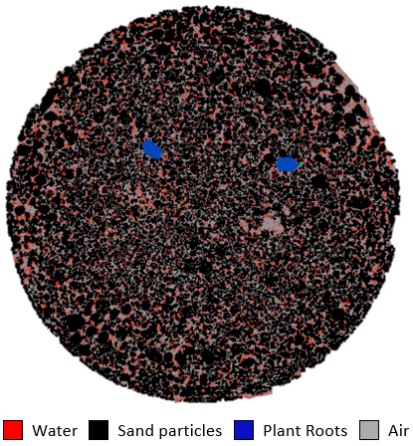

Figure 6. Segmented slice indicating the four different phases within the sample.

3.2. Local Digital Volume Correlation

Digital volume correlation (DVC) has to be considered as the well-known Digital Image Correlation procedure applied to a greyscale 3D volume. Correlation occurs between two images representing usually a reference status and a deformed status. In the specific case correlation is applied between two different stages of plant growth and water content. The Software for Practical Analysis and Measurements (SPAM) is used to run the DVC (Stamati et al., 2020). As mentioned before, the pixel size is 45 µm, not large enough to have the needed texture to run a particle scale correlation. A local approach is applied, single cubical subvolumes are defined in both reference and deformed images, using a regular grid to subdivide the greyscale 3D image in equal elements. The correlation aims to measure the linear deformation function (Φ), expressed as a 4x4 matrix. Φ encodes the displacement, rotation, stretch and shears of each subvolume (Birmpilis et al., 2022).

Considering the fact that each sample has been placed daily in the tomograph and due to the pixel resolution, the

whole set of images needed a rigid registration, in order to have unique reference coordinates and axes in each 3D images of the set.

4. Results

4.1. Soil Porosity

The segmentation of the soil phase not only helps to detect the soil particles, but also allows the understanding of possible fluctuations of the bulk porosity. This property is quantified based on (i) the vertical settlements recorded on the free surface, (ii) the rearrangement of the pore macro-structure within the medium.

The investigation of the soil porosity is initially done at the macroscale. The bulk porosity of the soil sample is quantified using the binarized segmented image of the soil matrix. Figure 7 shows the comparison between the trend of the bulk porosity (ratio of void volumes to total volume) and the volumetric water content (ratio of water volume to soil volume). The plot area is divided in four main subparts indicating the different water cycles components. The comparison of these two macro parameters shows an opposite trend. As VWC drops, porosity increases and vice versa. The first and the last observation days have same water content, but porosity shows an overall increase of 0.7% due to water cycle.

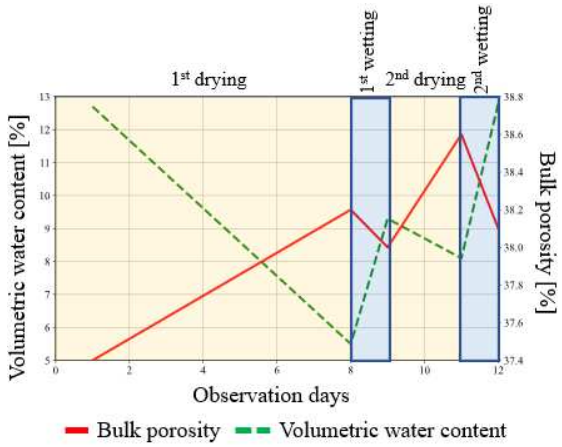

Figure 7. Comparison between volumetric water content and the porosity, during the drying (yellow area) and the wetting (blue area) cycles imposed on the sample.

To further investigate the porosity in the sample, the local porosity is measured along the depth. One value of porosity is measured every 10 slices within a trinarised version of the image (pore + solid + root). The porosity values at each depth are collected and plotted. For each stage of the water cycles and the plant growth, the porosity profile is obtained, as shown in Figure 8. In Figure 8 each plot shows the porosity profile comparison between two consecutive water content steps. Figure 8a shows the difference of porosity during the first drying cycle (i.e. from a wc of 12.9% to 5.6%), with an increase of porosity of 0.7%. Figure 8b shows that when increasing the water content again to 9.5%, the bulk porosity decreases of 0.2%. Figures 8c show that when the water content drops from 9.5% to 8.5% the porosity increases of 0.6%, while when the water content is brought back to the initial value of 12.9%, the porosity has an further decrease of 0.5% (Figure 8d). Three main observations arise from the plots (i) after drying-wetting cycles, for the same value of VWC, larger porosity is observed (see Figure 8e); (ii) induced wetting compacts the soil, while induced drying expands it; (iii) the increase in porosity during the wetting is larger in value than the decrease in porosity during drying. The first point of the list can be clearly seen comparing the two green curves, in Figure 8e, corresponding to initial and final time lapse of the observation, where the water content is the same, but the porosity differs.

4.2. Soil displacements

The observed variation in porosity impacts the kinematic response of the soil. The change in water content and growth of the root system leads to the evolution of the pore-microstructure. This modification of the pore connection and particle position can be quantified. Using local DVC, the displacements of soil subvolumes are obtained. Each subvolume has 18 px per side, and its position is tracked in each tomography.

An example of the output of the DVC is shown in Figure 9, where each vector represents the magnitude of the displacement of one specific subvolume. The vectors of the field are scaled and colored based on their magnitude. Three different status are compared: (i) reference state is the day 0 of observation, when no root was still in the sample; (ii) day 8 of observation, when the minimum water content was achieved; (iii) day 12 of observation, when the second wet cycle brought back the sample at the initial (highest) water content.

The DVC between day 0 and day 8, shows two main sources of displacements. First, around the primary root the block of soil (Figure 9 left) it is displaced mostly towards the bottom (whiter arrows around the green root). Second, within the core of the sample there is a clear displacement (light blue vectors) due to the rearrangement of the soil matrix caused by drying of the pores. The main phenomenon inducing displacement is the growth of the maize primary root, but significant displacement is also recorded far from the root, where macropores broke down into micropores leading to the soil particles rearrangement. The DVC observed between day 8 and day 12 (Figure 9 right) is induced by a wetting-drying-rewetting cycle. In this time period, particle displacements seem to be driven by water uptake from the two roots, while soil far from the root displaces randomly. It is worth noting the magnitude of the quantified displacements. In this second vector field,are present more vectors with a red color, indicating that many more subvolumes have registered a displacement of magnitude between 1 and 1.2 mm. To better understand the distribution and difference in magnitude of the displacements, we focus on the z component of the displacement vector. The two vertical slices in Figure 10 compare the displacement along the z axis between the reference state and day 8, as well as the reference state and day 12. We notice an accumulation of negative vertical displacements (i.e. towards the top of the sample) near the root body and at the bottom of the container. This local uplifting of the soil subvolumes can be associated to the capillary forces induced by the root water uptake

and by the evapotranspiration forced within the pore structure. The trend of the vertical component of the displacement helps understanding the overall porosity variation recorded at the bulk level (Figure 7).

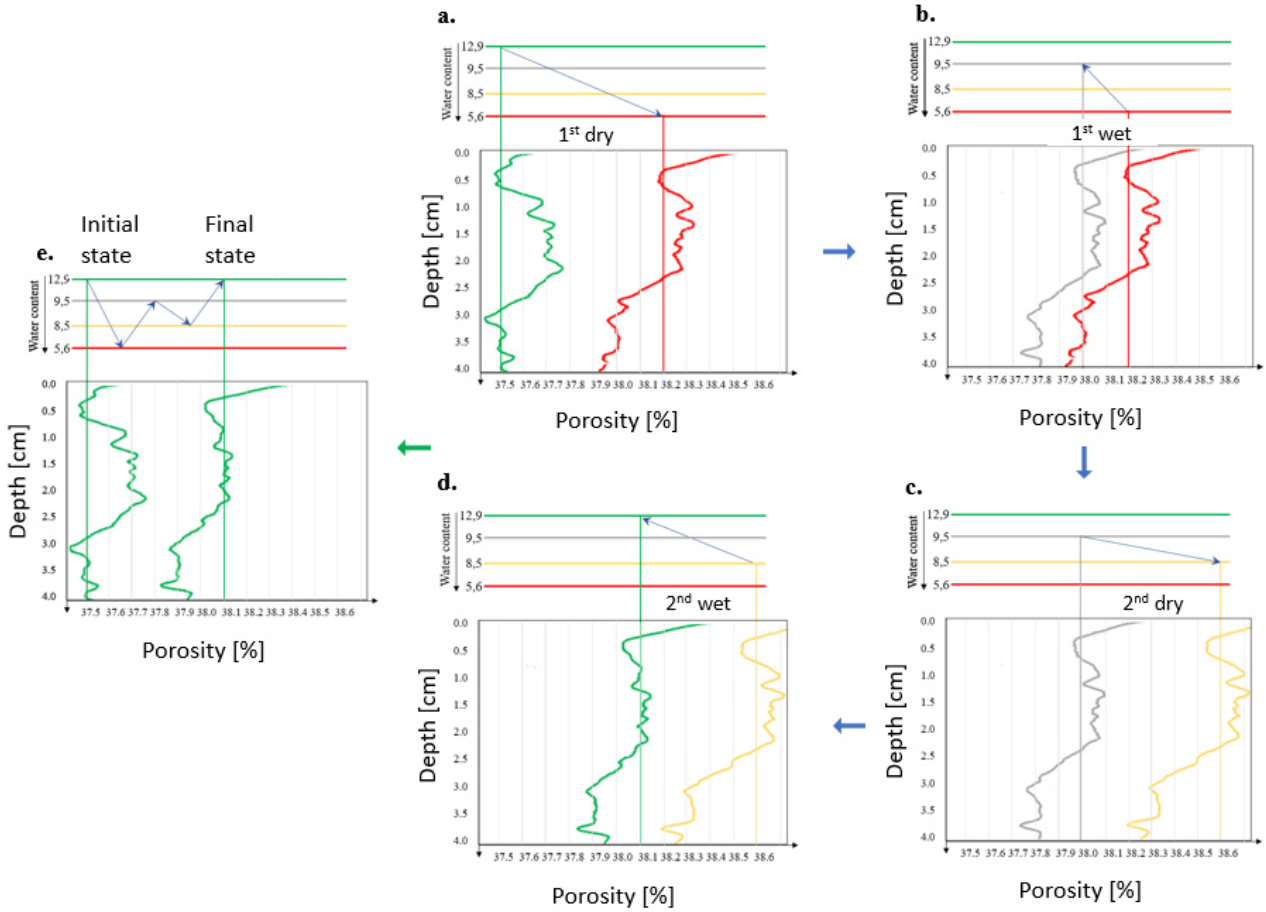

Figure 8 Comparison between the porosity profiles during the DWDW cycle.The straight line crossing each curve indicates the bulk density of the sample with that specific water content. On the top of each plot (a.-e.), the step of the water cycle is indicated. Plots a.-d. show the porosity profile of the same vegetated sample in two consecutive water content conditions. The arrow indicated the order of the water cycle and consecutive the porosity variation (increase a.-c., and decrease b.-d.). Plot e. shows the comparison between the initial and the final state of the sampe after the entire water cycle. The bulk water content is the same, but the entire water cycle process has affected the porosity profile, inducing a bulk dilation.

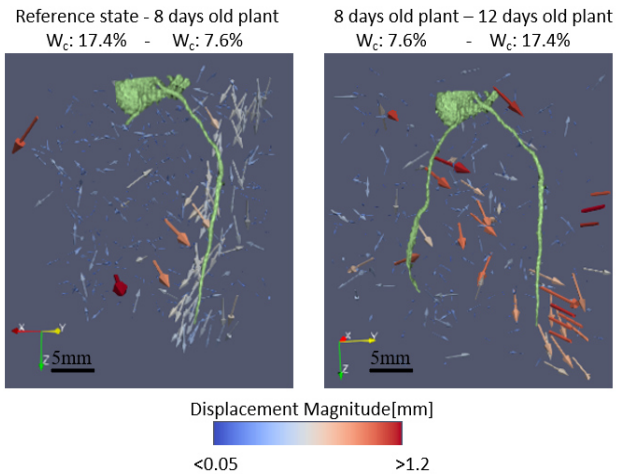

Figure 9. Vector field showing the magnitude of the displacement quantified with local digital volume correlation. The orientation of the vectors indicates the magnitude of the displacement. The size and the color of the arrows depend on the values of displacement related to the soil subvolume. The 3D root system is shown in green, at the 8th day and 12th day of growth, respectively, on the left image and the right image.

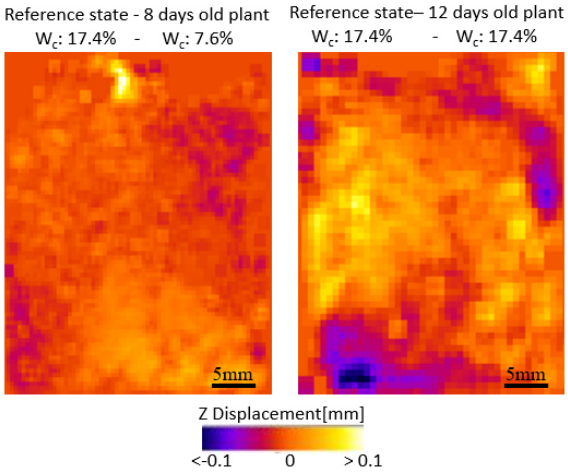

Figure 10. Vertical slices representing the displacement along the z-axis between day 0 and day 8 (left), and day 8 and day 12 (right). Each pixel shows the displacement value of one subvolume of 18px in size of the raw greyscaled image. The darker values of the colormap indicate negative displacements, the lighter color the positive displacements. The positive convention of the z-axis points downwards.

5. Conclusions

3D images obtained with x-ray microtomography of vegetated sand are used to quantify the microstructure variation of the vadose zone subjected to water drying-wetting cycles. On the soil evolution, the research has shown how the microstructure evolves as the water content changes, also in areas far from the root growth. The well-connected macropores at the interface with the container wall creates a preferential way for the root system to develop. During root growth a soil displacement of around 0.5 mm is quantified in its vicinity. The comparison between initial and final states shows displacements up to 1.2 mm, close and far from the root position.

The impact of wetting-drying cycles on the bulk porosity of sandy soil is significant. The anticipated "breathing" phenomenon of soil expanding and contracting as it dries and becomes wet again is not observed. However, it appears that extended periods of drying after a rewetting can still cause shifts within the structure of the soil. The global micro-structure rearrangement due to the double effects of plant water uptake and induced drying-wetting cycles translates into a bulk porosity increase. Specifically, these observation show that drying cycles increase porosity, whereas wetting cycles reduce it. After 12 days of observation, for the same water content, the bulk porosity changed from 37.4% to 38.1%. As described in Anselmucci et al 2021a, in sandy soil root growth induces a dilatant volumetric response. Therefore, the apparent increase in porosity is caused by the combination of wetting-drying water cycles, and the dilatancy due by the shear induced from the plant root growth.

As mentioned in the description of the methodology, during the experimental campaign, some of the samples were equipped with tensiometer and moisture sensors. SWRCs were constructed at different plant stages to quantify the impact of vegetation on soil suction. However, because the measurements of these instruments are influenced by the surrounding conditions, we cannot confirm, yet, that the differences in the soil water retention curves are solely due to the quantity of roots in the samples. Further investigations are needed to link SWRCs to pore size distribution and root quantity. The methodology and protocols presented in this work will be applied to an extension of this investigation, focusing on the local soil response to root growth and hydraulic cycles. Additionally, these investigation will provide validation for numerical simulation to enrich the state-of-the-art on root-soil interaction.

Acknowledgements

This work benefited from EPOS-NL facility access to the MINT x-ray tomography facilities at Delft University of Technology. See www.EPOS-NL.nl.

References

Anselmucci, F., Andó, E., Viggiani, G., Lenoir, N., Peyroux, R., Arson, C. and Sibille, L., 2021. "Use of X-ray tomography to investigate soil deformation around growing roots." *Géotechnique Letters*, *11*(1), pp.96-102, https://doi.org/10.1680/jgele.20.00114

Anselmucci, F., Andò, E., Viggiani, G., Lenoir, N., Arson, C. and Sibille, L., 2021. "Imaging local soil kinematics during the first days of maize root growth in sand." *Scientific reports*, *11*(1), pp.1-13, http://doi.org/10.1038/s41598-021-01056-1

Birmpilis, G., Andò, E., Stamati, O., Hall, S.A., Gerolymatou, E. and Dijkstra, J., 2022. "Experimental quantification of 3D deformations in sensitive clay during stress-probing." *Géotechnique*,1-12, https://doi.org/10.1680/jgeot.21.00114

Byrne, B.W., Schupp, J., Martin, C.M., Maconochie, A., Oliphant, J. and Cathie, D., 2013. "Uplift of shallowly buried pipe sections in saturated very loose sand." *Géotechnique*, *63*(5), pp.382-390, https://doi.org/10.1680/geot.11.P.016A

Chae, B.G. and Kim, M.I., 2012. "Suggestion of a method for landslide early warning using the change in the volumetric water content gradient due to rainfall infiltration." *Environmental Earth Sciences*, *66*(7), pp.1973-1986, http://doi.org/10.1007/s12665-011-1423-z

Cheng, H., Anselmucci, F.A., Fan, X., Zeng, Y., Luding, S. and Magnanimo, V., 2022. "Down to the root of vegetated soil: challenges and state-of-the-art." *Papers in Physics*, *14*, pp.140014-140014, http://doi.org/10.4279/PIP.140014

Colenbrander, H. J., Blumenthal, K. P., Cramer, W., and Votker, A., 1989. "Water in the Netherlands." T N O Committee on Hydrological Research, The Hague, The Netherlands. Proceedings and Information no. 37.

Laloui L. 2013 "Editorial: bio- and chemo-mechanical processes in geotechnical engineering." Géotechnique 2013 63:3, 189-190, https://doi.org/10.1680/geot.2012.63.3.189

Selker, J.S., McCord, J.T. and Keller, C.K., 1999. *Vadose zone processes*. CRC Press.

Stamati, O., Andò, E., Roubin, E., Cailletaud, R., Wiebicke, M., Pinzon, G., Couture, C., Hurley, R., Caulk, R., Caillerie, D. and Matsushima, T., 2020. "Spam: software for practical analysis of materials." *Journal of Open Source Software*, *5*(51), pp.2286, http://doi.org/10.21105/joss.02286

Tohari, A., Nishigaki, M. and Komatsu, M., 2007. "Laboratory rainfall-induced slope failure with moisture content measurement." *Journal of Geotechnical and Geoenvironmental Engineering*, *133*(5), pp.575-587, http://doi.org/10.1061/ASCE1090-02412007133:5575

Tomasi, C. and Manduchi, R., 1998, January. "Bilateral filtering for gray and color images." In *Sixth international conference on computer vision (IEEE Cat. No. 98CH36271)* (pp. 839-846). IEEE.